Supporting Information

Silvestre et al. 10.1073/pnas.1304045110

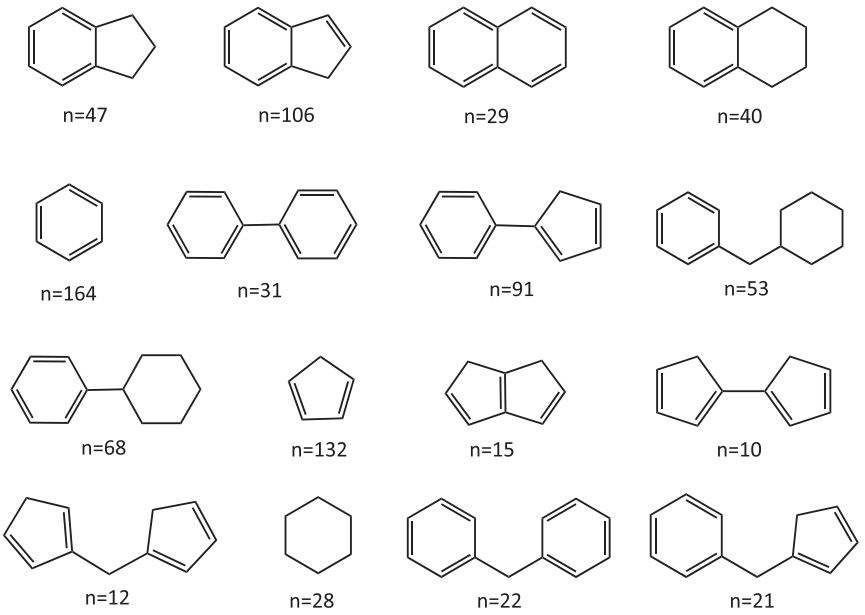

Fig. S1. The structural diversity present in the library used. Graph representation of the scaffolds present, accounting for 70% of the library. The atoms depicted can be assumed to be carbon, nitrogen, oxygen, or sulfur.

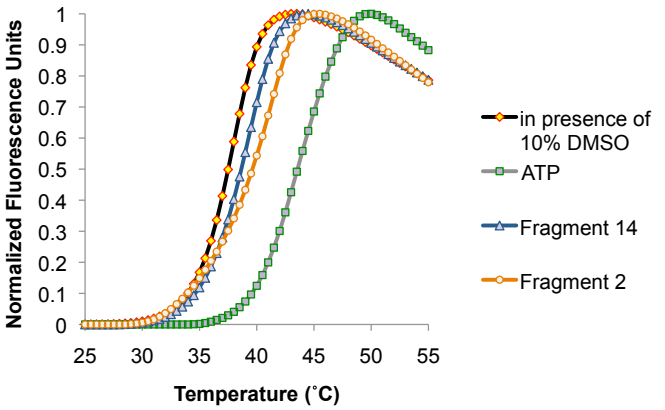

Fig. S2. The thermal unfolding of pantothenate synthetase (*Pts*). The thermal unfolding of *Pts*, in presence of 10% (vol/vol) DMSO, clearly depicts a two-state transition. This behavior is also observed in the presence of substrate (ATP) as well as fragments (as example).

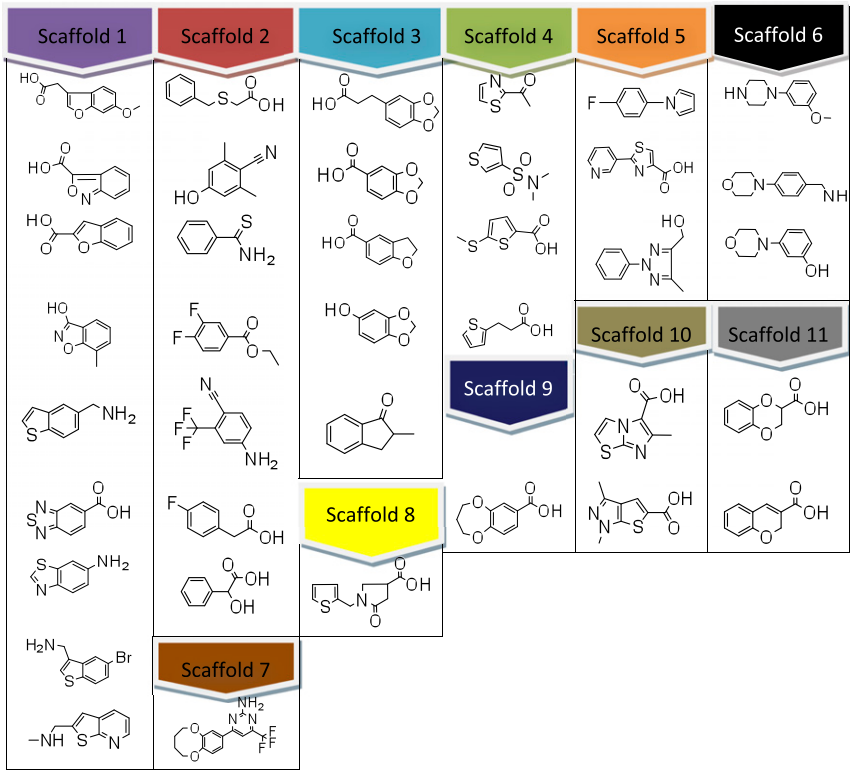

Fig. S3. The 39 fragments found by thermal shift. The hits are classified according to their scaffolds.

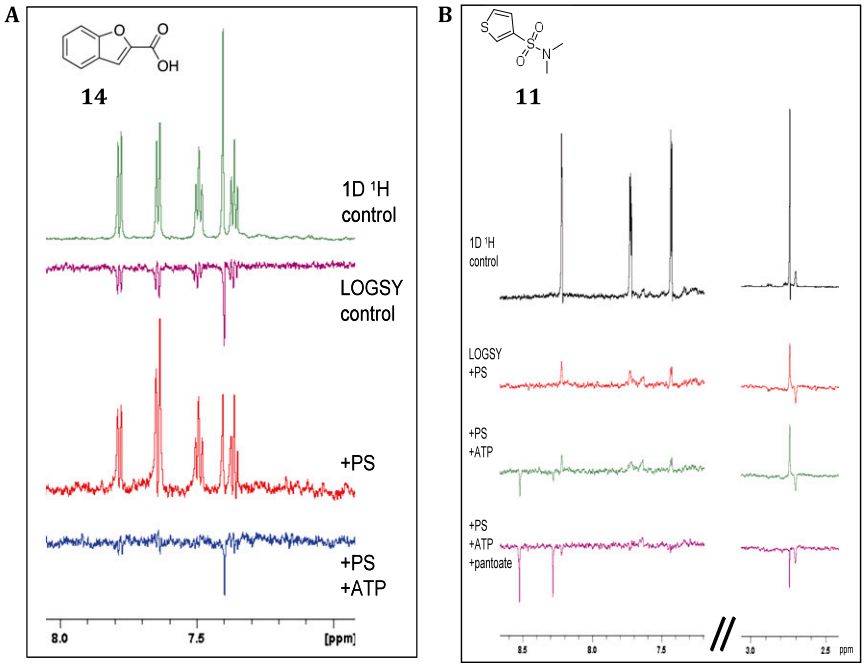

Fig. S4. Water ligand observed gradient spectroscopy NMR experiments to validate fragment binding. Displacement of fragment **14** upon addition of ATP (*A*), whereas fragment **11** (*B*) is not displaced upon addition of ATP only but is displaced upon subsequent addition of pantoate.

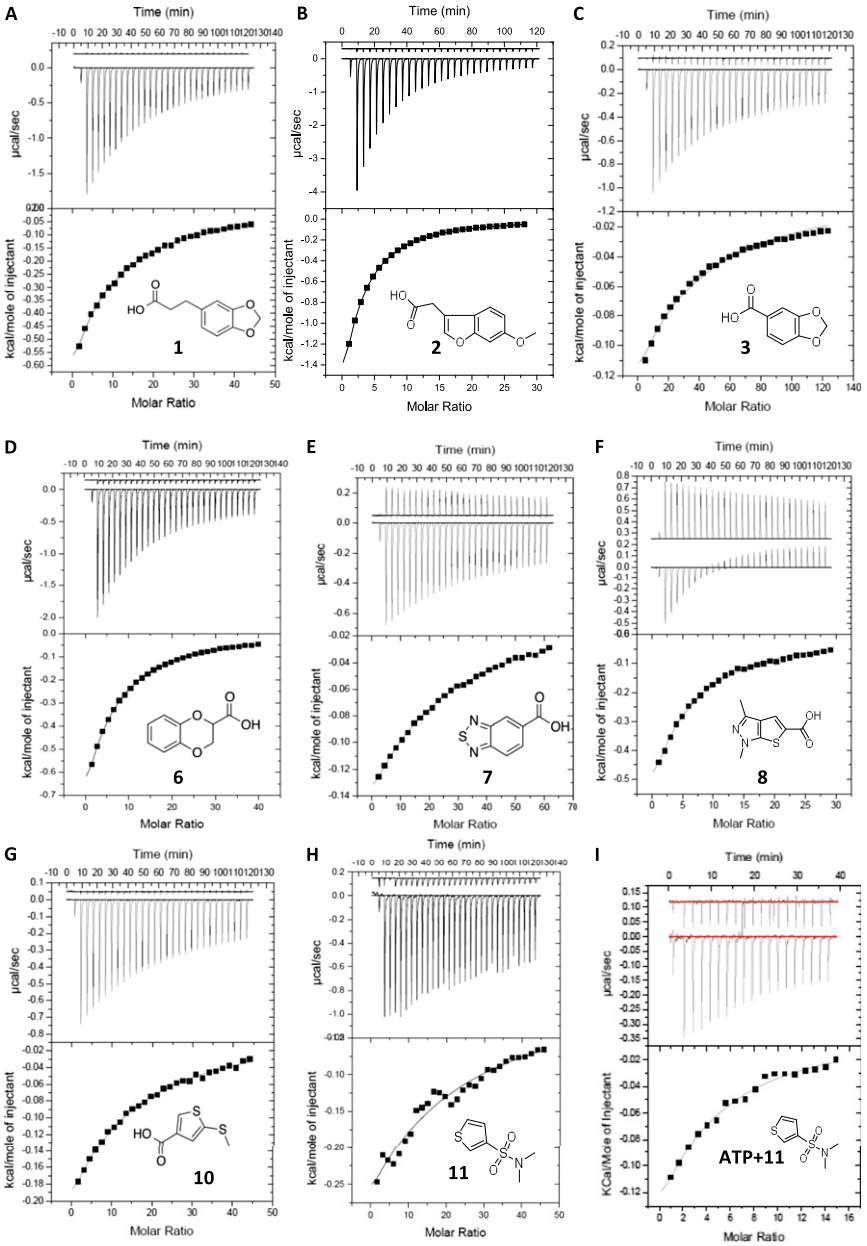

Fig. S5. (Continued)

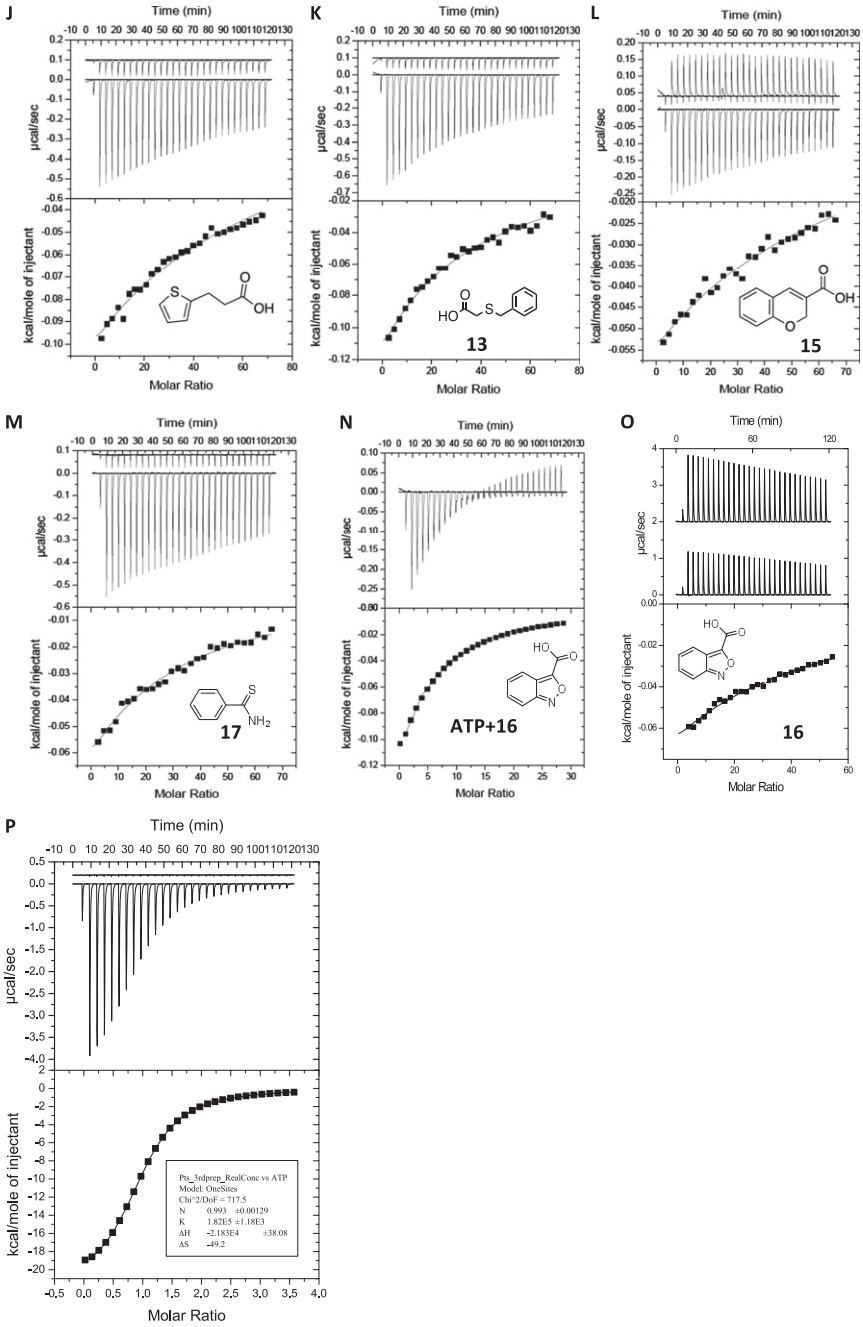

Fig. S5. Binding isotherms for 14 of the 17 fragments validated by NMR. For all panels (*A*–*O*), the top isotherm represents the heat of dissolution of the fragment in solution, whereas the second isotherm represents the *Pts*–fragment binding titration. *P* depicts a binding isotherm of *Pts*–ATP, which allows the accurate determination of protein concentration, necessary to draw correct conclusions for titrations under low *c*-values.

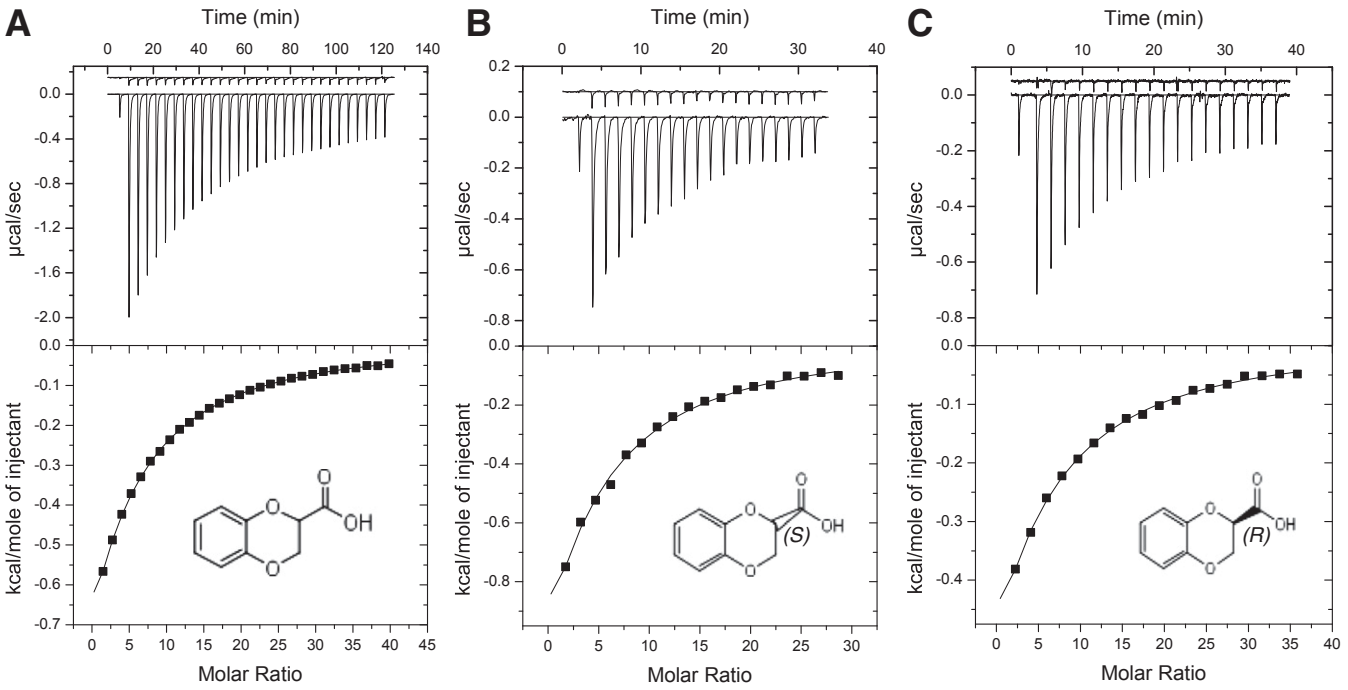

Fig. S6. Titrations of *Pts* with racemic and the corresponding enantiopure fragment **6**. The binding isotherm for the racemate mixture of **6**, the *S*-enantiomer, and the R-enantiomer are depicted in *A*, *B*, and *C*, respectively. The *S*-enantiomer exhibited slightly higher affinity (K_d of 670 μM). The resulting difference in affinity between the two enantiomers is 1.3-fold.

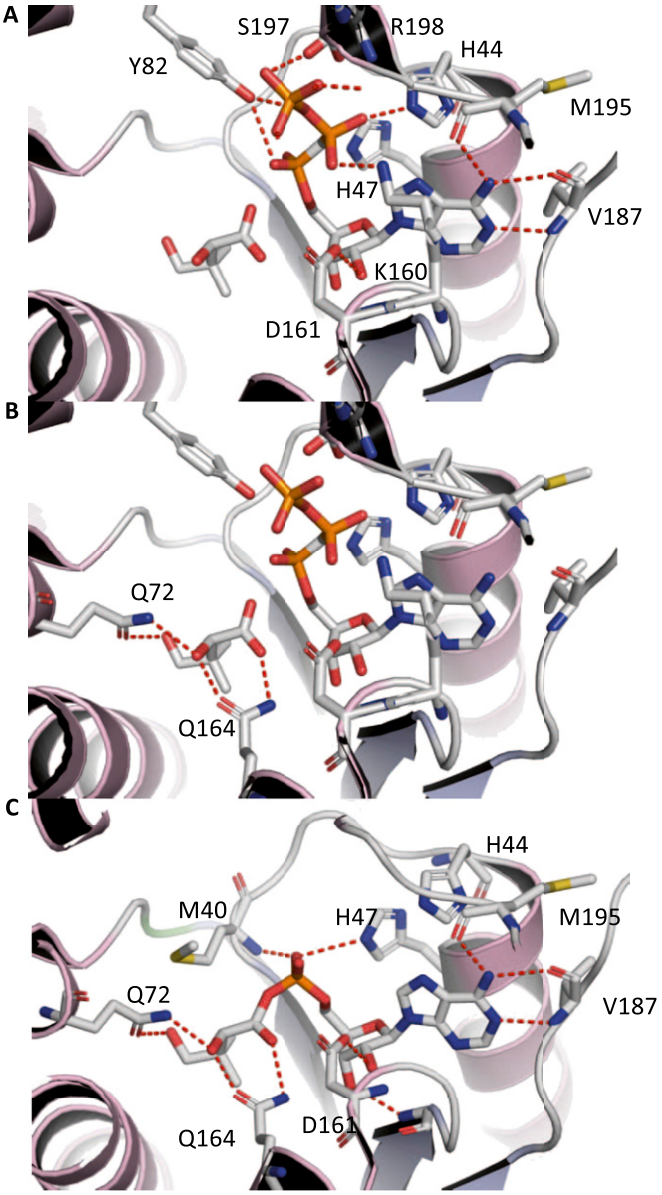

Fig. S7. *Pts* bound with the intervening substrates. In *A*, AMPCPP, in *B*, pantoate, and in *C*, the reaction intermediate pantoyladenylate are shown bound to *Pts*. The hydrogen bonds thought to be participating between the intervening substrates and *Pts* are highlighted in red.

Table S1. Physicochemical properties of the fragment library used in this study

Physicochemical properties	Average	SD	Rule of three
Molecular weight, Da	185.0	39.1	<300
Polar surface area, Å^2	39.4	13.4	≤60
Number of rotatable bonds	1.85	1.15	≤3
Hydrogen bond acceptor	2.64	1.57	≤3
Hydrogen bond donor	1.23	1.10	≤3
LogP	1.51	0.99	≤3

Table S2. Crystallographic data collection and refinement statistics for all new fragment-bound crystal structures resulting from this study and deposited in the Protein Data Bank

	Fragment **1**	Fragment **2**	Fragment **3**	Fragment **6**	Fragment **8**	Fragment **7**	Fragment **11**	Fragment **11** + ATP
Data Collection								
Protein Data Bank ID code	4EF6	4DDH	4DDK	4G5F	4FZJ	4DDM	4EFK	4G5Y
X-Ray Source	SLS, PXIII	SLS, PXIII	ESRF, ID14-1	SLS, PXIII	DLS, I03	SLS, PXIII	ESRF, ID29	ESRF, ID29
Space Group	$P2_1$	$P2_1$	$P2_1$	$P2_1$	$P2_1$	$P2_1$	$P2_1$	$P2_1$
Cell Parameters ($\alpha=\gamma=90^0$)								
a (Å)	48.12	48.62	48.19	48.41	48.29	48.44	48.45	48.26
b (Å)	70.70	70.95	70.71	70.99	70.90	71.02	71.78	71.06
c (Å)	82.11	82.00	81.69	81.68	81.83	82	81.91	81.65
β°	99.40	99.40	99.14	99.58	99.54	99.5	99.55	99.35
Resolution range, Å (outer shell)	38–1.94 (2.04–1.94)	53.3–2.07 (2.16–2.07)	26.58–1.75 (1.84–1.75)	47.73–2.33 (2.46–2.33)	53.26–1.63 (1.72–1.63)	28.61–1.85 (1.95–1.85)	30–1.7 (1.74–1.70)	40.28–1.80 (1.90–1.80)
No. of unique reflections	40,119	34,573	49,951	23,179	66,694	46,927	60,243	50,752
Multiplicity	4.2	4.4	2.9	3.6	2.6	4.5	3.5	4.1
R_{merge} % (outer shell)	11.5 (66.8)	12.3 (54.5)	7.9 (42.7)	11.3 (47.7)	7.3(59.6)	6.5 (46.8)	6.1 (42.8)	5.4 (37.2)
Average I/σ (I)	12 (1.7)	13.8 (3.8)	7.9 (2.4)	7.5 (2.6)	8,2 (1.8)	17 (2.9)	12.8 (2.1)	15.3
Completeness % (outer shell)	99.5 (96.5)	99.8 (99.9)	91.5 (89.5)	(98.6) 90.7	98.2 (98.4)	100 (100)	99.0 (91.0)	99.6 (99.3)
Mosaicity, °	0.65	0.65	0.6	1.2	0.33	0.7	0.48	0.21
Wilson B, $Å^2$	20.5	23	16.1	31.7	19	22.51	29.8	31.2
Refinement								
Resolution range	81.11–1.94	80.85–2.07	80.58–1.75	80–2.33	80.85–1.63	80.85–1.85	80.99–1.7	37.57–1.80
R_{cryst}, %*	0.17	0.19	0.18	0.17	0.17	0.16	0.17	0.16
R_{free}, %†	0.22	0.25	0.24	0.23	0.21	0.22	0.21	0.21
Number of reflections								
Working set	38,082	31,737	47,412	21,974	63,290	45,985	35,104	48,205
Test set	2,634	1,694	2,371	1,191	3,382	3,385	1,846	2,542
Ligands bound to active site								
Water molecules	489	487	565	232	448	249	391	404
Ligand	2	2	2	2	1	2	2	2
Glycerol	5	2	4	2	1	1	3	2
Ethylene glycol	3	2	1	2	1	1	0	0

DLS, Diamond Light Source; ESRF, European Synchrotron Radiation Facility; PXIII, Protein Crystallography III (refers to the beam station from where the data was collected, analogous to "ID14-1"); SLS, Swiss Light Source.

*$R_{cryst} = \Sigma||F_{obs}|-|F_{calc}||/\Sigma|F_{obs}|$, and F_{obs} and F_{calc} are observed and calculated structure factor amplitudes.

†R_{free} as for R_{cryst} using a random subset of the data excluded from the refinement.